

Condensed Matter and Interphases

Kondensirovannye Sredy i Mezhfaznye Granitsy
<https://journals.vsu.ru/kcmf/>

Original articles

Research article

<https://doi.org/10.17308/kcmf.2022.24/9053>

The influence of the physicochemical nature of the components of the V_2O_5 /GaAs, MnO_2 /GaAs, V_2O_5 /InP, MnO_2 /InP, TiO_2 /InP, and SnO_2 /InP heterostructures and the oxidation conditions on the surface morphology of the synthesised films

A. S. Kovaleva¹✉, B. V. Sladkoptsev¹, A. A. Samsonov¹, S. I. Alferova², D. G. Kovalev¹, S. A. Titov¹, N. D. Pryakhin¹, I. Ya. Mittova¹

¹Voronezh State University,

¹Universitetskaya pl., Voronezh, 394018, Russian Federation

²Voronezh State Pedagogical University,

86 ul. Lenina, Voronezh, 394043, Russian Federation

Abstract

The formation of oxide functional films on the surface of semiconductors is a serious technological challenge, which is even more complicated in the nanometre thickness range. It is necessary to form films with specified values of thickness, resistivity, and a certain surface morphology for practical applications. Such films are used in micro- and optoelectronics, environmental monitoring, and alternative energy devices. The goal of this work is to establish the features of the surface morphology of thin films formed as a result of the thermal oxidation of the MnO_2 /GaAs, V_2O_5 /GaAs, V_2O_5 /InP, MnO_2 /InP, TiO_2 /InP, and SnO_2 /InP heterostructures depending on the physicochemical nature of the components and the oxidation conditions.

The synthesis of thin films on the InP and GaAs surfaces was carried out by thermal oxidation under the influence of magnetron-deposited layers of chemostimulator-modifiers. The thickness of the formed films and their composition were determined by laser ellipsometry, X-ray phase analysis, and infra-red spectroscopy. The scanning tunnel and atomic force microscopy were used to determine the morphological characteristics of the films and their dependence on the type of semiconductor substrate, the nature of the chemostimulator-modifier, and the conditions of the thermal oxidation.

The application to the GaAs and InP surfaces of the most effective chemostimulator-modifiers (V_2O_5 and MnO_2) of thermal oxidation and higher temperatures of the oxidation process contributed to the formation of smoother and nanostructured films.

Keywords: Gallium arsenide, Indium phosphide, Heterostructure, Thermal oxidation, Surface morphology, Grain size

Acknowledgements: The research results were partially obtained using the equipment of the Centre for Collective Use of Scientific Equipment of Voronezh State University. URL: <http://ckp.vsu.ru>

For citation: A. S. Kovaleva, B. V. Sladkoptsev, A. A. Samsonov, S. I. Alferova, D. G. Kovalev, S. A. Titov, N. D. Pryakhin, I. Ya. Mittova The influence of the physicochemical nature of the components of the V_2O_5 /GaAs, MnO_2 /GaAs, V_2O_5 /InP, MnO_2 /InP, TiO_2 /InP, and SnO_2 /InP heterostructures and the oxidation conditions on the surface morphology of the synthesised films. *Kondensirovannye sredy i mezhfaznye granitsy = Condensed Matter and Interphases*. 2022;24(1): 33–44. <https://doi.org/10.17308/kcmf.2022.24/9053>

Для цитирования: Ковалева А. С., Сладкопцев Б. В., Самсонов А. А. Алферова С. И., Ковалев Д. Г., Титов С. А., Пряхин Н. Д., Миттова И. Я. Влияние физико-химической природы компонентов гетероструктур MnO_2 /GaAs, V_2O_5 /GaAs, V_2O_5 /InP, MnO_2 /InP, TiO_2 /InP и SnO_2 /InP и режима процесса оксидирования на морфологию поверхности синтезированных пленок. *Конденсированные среды и межфазные границы*. 2022;24(1): 33–44. <https://doi.org/10.17308/kcmf.2022.24/9053>

✉ Anastasia S. Kovaleva, e-mail: nkovaleva.vsu@yandex.ru

© A. S. Kovaleva, B. V. Sladkoptsev, A. A. Samsonov, S. I. Alferova, D. G. Kovalev, S. A. Titov, N. D. Pryakhin, I. Ya. Mittova, 2022



The content is available under Creative Commons Attribution 4.0 License.

1. Introduction

The synthesis of new materials for electronics has always been important. They have been used to create competitive optoelectronic [1], environmental monitoring [2], and alternative energy [3] devices. The challenges of import substitution and miniaturisation require new highly rapid, environmentally friendly, and cost-effective methods and approaches to create efficient devices based on MIS (metal-insulator-semiconductor) and SIS (semiconductor-insulator-semiconductor) structures [4–7]. Thermal oxidation is one of the most common methods used to create nanosized functional oxide films on the surface of semiconductors [8]. This technological challenge becomes more complicated in the nanometre thickness range since in many processes the regular growth of films begins at a sufficiently developed stage (at a thickness of more than 100 nm) and the dependence of film properties on their surface morphology and structure is the most pronounced in the nanometre thickness range.

The intrinsic thermal oxidation of the A^3B^5 semiconductors leads to the formation of low quality films, which can be improved by changing the process mechanism from intrinsic to chemically stimulated [8, 9]. Nanoscale layers of oxide-chemostimulators, formed by the method of reactive magnetron sputtering contribute to a change in the mechanism of the oxidation of GaAs and InP semiconductors from intrinsic to transit or catalytic, which allows accelerating the process of film growth, purposefully changing their composition, surface morphology, and structure and, consequently, their properties [9].

In [10–13], it was established that nanosized layers of V_2O_5 [10, 11] applied to the InP and GaAs surfaces contribute to catalytic oxidation, whereas the application of nanosized layers of MnO_2 [12, 13] mainly promote transit oxidation. Coated layers of SnO_2 [14, 15] and TiO_2 [16, 17] do not exhibit chemical stimulating properties in the processes of InP thermal oxidation, although they are thermodynamically capable of transferring oxygen to semiconductor components; however, they modify the composition of the film.

The investigation of the surface morphology of films formed as a result of thermal oxidation of heterostructures based on A^3B^5 semiconductors

is necessary in order to track the dynamics of changes in their characteristics compared to reference samples, to understand the dependence of the surface morphology of synthesised objects on the physicochemical nature of the substrate and deposited oxide, the oxidation conditions, and the characteristics of films. Such data are necessary to optimise the formation of low-dimensional composite structures based on A^3B^5 semiconductors, primarily MIS structures. It is assumed that the created oxide films can compete with SiO_2 when manufacturing ohmic contacts, anti-reflective coatings for mirrors of heterolasers on GaAs and InP substrates, and in other aspects of functional electronics [4, 7].

Therefore, the goal of this work is to establish the features of the surface morphology of thin films formed as a result of thermal oxidation of the V_2O_5 /GaAs(100), V_2O_5 /GaAs(111), MnO_2 /GaAs(100), MnO_2 /GaAs(111), V_2O_5 /InP, MnO_2 /InP, TiO_2 /InP, and SnO_2 /InP heterostructures depending on the physicochemical nature of the components and the oxidation conditions.

2. Experimental

As semiconductor substrates, we used pre-prepared (100) and (111) oriented AGChT (tellurium-doped, electronic) gallium arsenide with a concentration of the main charge carriers of at least $8 \cdot 10^{18} \text{ cm}^{-3}$, and (100) oriented FIE-1A (tin-doped, electronic) indium phosphide with a concentration of the main charge carriers of at least $5 \cdot 10^{16} \text{ cm}^{-3}$.

When studying the mechanisms of processes on the surface and in layers of nanometre thickness, it is necessary to pay special attention to the standardisation of the surface morphology of the substrates, which dictates a thorough pretreatment of monocrystals. Before thin-film heterostructures were formed, the used substrates were treated with the following etchers: a) to clean and polish the surface of indium phosphide, we used a peroxide-sulphuric acid polishing solution $H_2SO_4:H_2O_2:H_2O = 2:1:1$, etching time was 10 min; b) to clean and polish the surface of gallium arsenide, we used concentrated hydrofluoric acid ($\omega(HF) = 49\%$), etching time was 10 min. The gallium face of GaAs(111) was determined by the method described in [18]. We needed to determine the gallium face of such a

substrate since it is more preferable for growing films on it: the film's microstructure would be less defective.

A thin nanosized (~35 nm) oxide layer performing a chemically stimulating (modifying) function was deposited by reactive magnetron sputtering of vanadium target (99.99% purity) with a diameter of 50 mm (2 inch) in an oxygen-argon atmosphere (V_2O_5 layers) using an Angstrom engineering CoVap II installation. The initial evacuation of atmospheric air from the vacuum chamber was carried out with a fore vacuum pump, and the subsequent deep evacuation ($p_{res} \sim 10^{-6}$ Torr) was conducted by a Varian Turbo 301 turbomolecular pump. In the process of developing a technique for sputtering a vanadium target in an oxygen-argon atmosphere, the optimal composition of the gas mixture was established for the reactive deposition of vanadium pentoxide layers Ar:O₂ – 3:1. Nanoscale layers of the SnO₂ modifier (Sn target with 99.99 % purity) and TiO₂ (Ti target with a purity of at least 99.8%) were deposited in similar way. The MnO₂ layers (a compressed target of manganese dioxide powder with a purity of at least 99.8 %) were deposited in an Ar atmosphere.

The first step in the study of various characteristics is to determine the composition of layers formed by magnetron sputtering on the surface of semiconductors. For HSs with V_2O_5 , the deposited layer mainly consisted of vanadium pentoxide but in addition to it, the diffraction patterns showed a peak corresponding to V_2O_3 , which can be explained by the specifics of the magnetron sputtering process. However, its relative content was low; therefore, we designated the synthesised HSs as V_2O_5/A^3B^5 [10]. A similar situation was characteristic of HSs with MnO₂: the magnetron-sputtered layer on A^3B^5 mostly consisted of MnO₂ with a relatively small inclusion of Mn₂O₃, therefore, we designated the synthesised HSs as MnO₂/ A^3B^5 [12,13]. Magnetron sputtering of tin dioxide on the InP surface resulted in the formation of a layer of SnO₂, without the formation of undesirable phases [14]. The titanium dioxide layer formed by magnetron sputtering only contained TiO₂ phases in structural modifications of anatase and rutile [19].

The thermal oxidation of synthesised heterostructures $V_2O_5/GaAs(100)$, $V_2O_5/GaAs(111)$, $MnO_2/GaAs(100)$, $MnO_2/GaAs(111)$, V_2O_5/InP , MnO_2/InP , TiO_2/InP , and SnO_2/InP was carried out in a flowing quartz reactor of a horizontal resistive heating furnace MTP-2M-50-500 (TRM-10 sensor unit, adjustment accuracy ± 1 °C) in flowing oxygen (the volume flow rate of 30 l/h) in the temperature range from 500 to 550 °C. The oxidation time varied between 20–180 minutes.

For practical applications, it is necessary to form films with specified values of thickness, resistivity, and a certain stable and reproducible surface morphology. MnO₂/GaAs and $V_2O_5/GaAs$ heterostructures with (100) and (111) oriented substrates were thermally oxidised in various conditions until the target film thickness of up to ~250 nm was reached. The formation of films with a thickness of about 200 nm was necessary to compare them with SiO₂ films of similar thickness, which are widely used to manufacture ohmic contacts, to protect side edges of mesastripes, and to create anti-reflective coatings for mirrors of Fabry-Perot heterolaser resonators on GaAs and InP substrates in a system of GaInAsP isolattice solid solutions covering the wavelength range of 0.8–1.8 μm [3]. A necessary requirement for the formed films is certain values of electrical strength, breakdown voltages, adhesion to the substrate, and surface roughness. The study of films of the nanoscale thickness range is natural due to the further miniaturisation of micro- and optoelectronic objects [6, 7].

The thicknesses of the deposited layers of chemostimulator oxides and films grown as a result of thermal oxidation were controlled by laser (LE, LEF-754, wavelength of 632.8 nm, ± 1 nm accuracy) and spectral ellipsometry (SE, Ellips-1891, wavelength range of 250–1100 nm, the measurement accuracy of the ellipsometric parameters $\Psi\delta = 0.05^\circ$ and $\delta\Delta = 0.1^\circ$). To interpret the measurement results, we used a single-layer model “external medium–film–substrate” with sharp interfaces between the media [20–22].

By increasing the growth rate of the film thickness as compared to the intrinsic oxidation (acceleration of the process), it is possible to judge whether the selected substance is a chemostimulator. A relative increase in the

growth rate of oxide film b during the thermal oxidation of HS was calculated by formula (1):

$$b = \frac{\Delta d_{\text{Me}_x\text{O}_y/\text{A}^3\text{B}^5}}{\Delta d_{\text{A}^3\text{B}^5}}, \quad (1),$$

where $\Delta d_{\text{A}^3\text{B}^5}$ is a change in the thickness of the oxide film during the intrinsic oxidation of the semiconductor (standard) and $\Delta d_{\text{Me}_x\text{O}_y/\text{A}^3\text{B}^5}$ is a change in the thickness of the oxide film during the thermal oxidation of the HS with a deposited chemostimulator layer minus the thickness of the latter [13].

To characterise the heterostructures and thin films formed on the semiconductor surface, a set of instrumental methods was used. The phase composition of the samples was studied by X-ray phase analysis (XPA) using a ARL X'tra diffractometer (Thermo Scientific, $\text{CuK}_{\alpha 1}$ with $\lambda = 1.540562 \text{ \AA}$). Data on the chemical bonds in the synthesised films were obtained by transmission infrared spectroscopy (IRS) using a VERTEX 70 IR-Fourier spectrometer (frequency range of $400\text{--}1400 \text{ cm}^{-1}$). The surface morphology of the samples and reference samples was studied by atomic force microscopy (AFM) using a Solver P47 Pro scanning probe microscope by NT-MDT corporation in the semi-contact mode at various points of the surface with an HA_NC Etalon cantilever and by scanning tunnelling microscopy (STM) using the NTK UMKA in the DC mode. These methods were complementary since the surface of dielectrics could not be studied by the STM method, and one of our tasks was to form dielectric oxide films.

3. Results and Discussion

The results of film thickness measurements (LE, SE) on GaAs monocrystal samples of various

orientations with nanoscale layers of MnO_2 and V_2O_5 chemostimulators at 500 and 530 °C in the time intervals from 20 to 180 minutes are given in Table 1.

Films with a thickness of less than 100 nm were synthesised most quickly on the $\text{V}_2\text{O}_5/\text{GaAs}(111)$ HS, which allows us to conclude that the time of film formation depends on the substrate orientation when the V_2O_5 HS is used as a chemostimulator. For the GaAs(111) orientation of the substrate, there was the largest bond angle between the surface atoms and the plane of the substrate surface (90°), which determined the bond availability for oxygen [18]. This contributed to a higher rate of interaction between the plane and the oxidiser. No such dependence was found for the MnO_2/GaAs heterostructure.

When comparing the thicknesses of the formed films for similar InP-based HSs (Table 2), it was obvious that there was a maximum acceleration when using the magnetron-formed layer of V_2O_5 as a chemostimulator. The layers of tin and titanium dioxides had the opposite effect; they slowed down the process of film formation during the oxidation of the heterostructure but acted as modifiers of the composition of oxide films (Table 3), which was necessary for the formation of films with the desired properties [14].

Films formed by thermal oxidation of the $\text{V}_2\text{O}_5/\text{GaAs}(100)$ HSs consisted of vanadium oxides in various oxidation states (V_2O_5 and VO_2) (Fig. 1a). This was related to the decomposition of V_2O_5 in flowing oxygen during thermal oxidation and the active interaction of vanadium pentoxide with substrate components. The VO_2 phases on the X-ray pattern of the sample with the substrate orientation (111) was not observed (Fig. 1b).

Table 1. Thicknesses of nanoscale films (LE, SE) formed by thermal oxidation of HSs on GaAs with deposited layers of V_2O_5 and MnO_2 in various conditions and the relative change in film thickness calculated by formula (1)

Sample	TO mode	Film thickness, nm		Relative change in film thickness, times
		LE	SE	
$\text{V}_2\text{O}_5/\text{GaAs}(100)$	$T=500 \text{ }^\circ\text{C}, t=50 \text{ min}$	83	81	2.18
$\text{V}_2\text{O}_5/\text{GaAs}(111)$	$T=500 \text{ }^\circ\text{C}, t=25 \text{ min}$	88	86	2.41
$\text{MnO}_2/\text{GaAs}(100)$	$T=500 \text{ }^\circ\text{C}, t=60 \text{ min}$	77	74	1.91
$\text{MnO}_2/\text{GaAs}(111)$	$T=500 \text{ }^\circ\text{C}, t=70 \text{ min}$	72	74	1.68
GaAs	$T=500 \text{ }^\circ\text{C}, t=60 \text{ min}$	27	27	–

Table 2. Thicknesses of films (LE) formed by thermal oxidation of HSs based on InP at 530 °C for 60 min and the relative change in film thickness calculated by formula (1)

Sample	TO mode	Film thickness, nm	Relative change in film thickness, times
SnO ₂ (68 nm)/InP	T=530 °C, t=60 min	82	0.389
TiO ₂ (35 nm)/InP		53	0.48
V ₂ O ₅ (21 nm)/InP		115	2.61
MnO ₂ (21 nm)/InP		76	1.5
InP		41	–

Table 3. Identified phases for GaAs-based HSs after thermal oxidation for 50 and 20 minutes, respectively, at 500 °C

Sample, TO mode	Interplane distance, d_{hkl}	Defined phase
V ₂ O ₅ /GaAs(100) (50 min)	4.3743; 3.1498	V ₂ O ₅
	3.3510	VO ₂
	3.2607; 1.4553	As ₂ O ₅
	2.1903	Ga ₂ O ₃
	2.0628	GaAs
V ₂ O ₅ /GaAs(111) (20 min)	4.3876; 2.7577	V ₂ O ₅
	2.0644	GaAs
	1.4531	As ₂ O ₅
	2.1770	Ga ₂ O ₃

No arsenates were found in the films since the conditions of thermal oxidation were not severe enough, however, gallium and arsenic oxides were present as had been expected (see Table 3). The XPA and IR methods also confirmed the absence of vanadium oxide consumption, i.e., the process of thermal oxidation of the studied HSs in various conditions had a catalyst regeneration cycle, which in our case was vanadium oxide (V) [8–10].

The presence of arsenic in the films in the form of As₂O₅ indicated the binding of the substrate components at the internal interface, which prevented the accumulation of underoxidised arsenic. A change in the orientation of GaAs at a constant temperature of thermal oxidation (500 °C) led to changes in the qualitative phase composition of the films. The X-ray pattern of the film grown by thermal oxidation of the V₂O₅/GaAs(100) HS had 2 reflections corresponding to As₂O₅, while the X-ray pattern of the film formed by the oxidation of V₂O₅/GaAs(111) had no second As₂O₅ peak, which indicated a more efficient binding of oxygen components in case of the (100) oriented substrate.

In case of the transition to other HSs, in which indium phosphide acted as a substrate, the composition of the films became somewhat more complicated. The formed films consisted of vanadium oxides in various oxidation states (V₂O₅; V₂O₃; VO₂), indium oxide (In₂O₃), and indium phosphate (InPO₄) (Table 4) [11]. The qualitative difference from similar gallium arsenide-based HSs was primarily that their X-ray pattern had peaks corresponding to indium phosphate, one of the target oxidation products for this particular semiconductor, formed as a result of the secondary interaction of the corresponding oxides. Using the data about the composition of the film formed on the SnO₂/InP HS, we can draw a conclusion about the modifying properties of SnO₂ [14]. The presence of peaks corresponding to the Sn₃(PO₄)₂ compound indicates an interaction between the SnO₂ layer deposited on the surface with the oxidation products of the substrate components, in particular phosphorus, and, as a consequence, a change in the composition of the film and its surface. Additional studies of the TiO₂/InP sample by IR spectroscopy revealed absorption bands

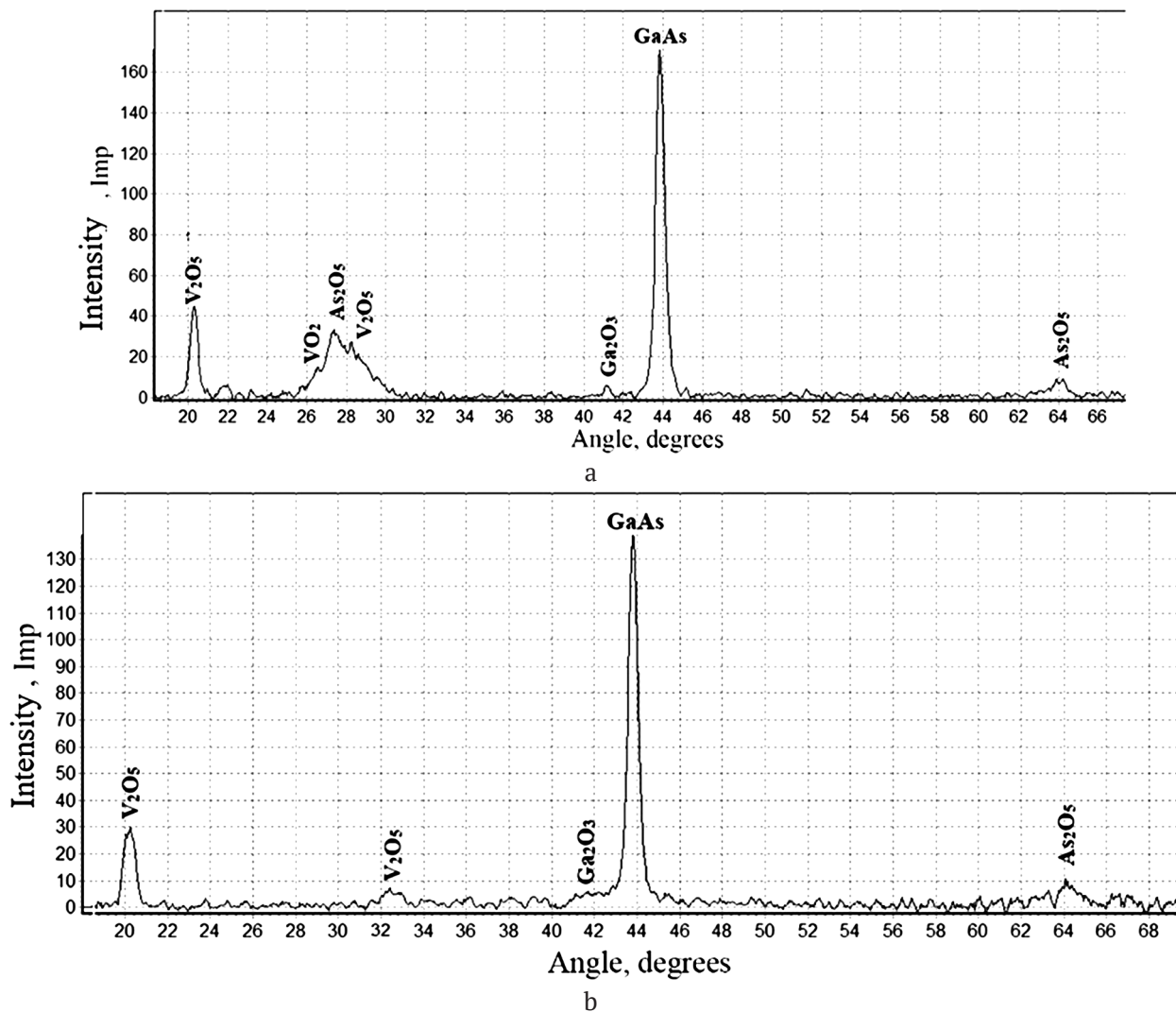


Fig. 1. XRD patterns of $V_2O_5/GaAs(100)$ (a) and $V_2O_5/GaAs(111)$ (b) heterostructures after thermal oxidation at a temperature of 500 °C for 50 minutes and 20 minutes, respectively

of the $Ti(PO_3)_3$, TiP_2O_7 , $Ti_4(P_4O_{12})_3$, $InPO_4$, and $In(PO_3)_3$ compounds [23,24], which also indicates the modifying effect of titanium dioxide layers.

The surface morphology of the synthesised nanosized films reflected the different nature of the effect of the deposited oxides. Thermal oxidation of HSs of $V_2O_5/GaAs$ (relief height within 10 nm) and $MnO_2/GaAs$ (relief height of 70 nm) for 50 and 60 minutes, respectively (Fig. 2), led to the formation of films with a pronounced grain structure with an average lateral grain size of 360 nm for $MnO_2/GaAs(100)$ and 150 nm for $V_2O_5/GaAs(100)$. The ordered arrangement of grains was most pronounced on the surface of the $V_2O_5/GaAs(100)$ sample.

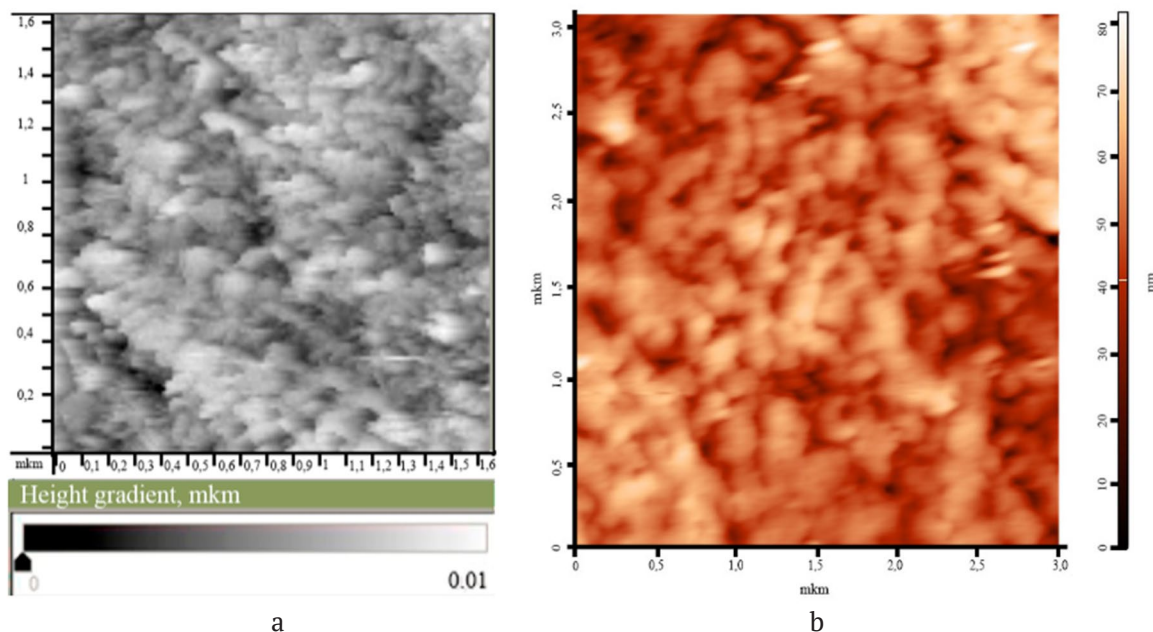
Films formed with a thickness of more than 130 nm had noticeable differences in the data

of laser and spectral ellipsometry, which can be associated with a greater development of the surface of the films with an increase in the oxidation time (according to AFM data, the maximum relief height reached 200 nm for the $MnO_2/GaAs(100)$ sample with an oxide film thickness of 232 nm according to the averaged LE and SE data (Fig. 3)). The films were characterised by a grain structure with an average diameter of the grain of 300 nm. There was a similar tendency to the formation of a more developed surface (relief height of 87 nm at a film thickness of 164 nm, average diameter of the grain of 250 nm) with an increase in the oxidation time for the $V_2O_5/GaAs(100)$ sample.

After 60 minutes of thermal oxidation of the V_2O_5/InP HS at 530 °C (the thickness of the formed

Table 4. Identified phases for the $\text{Me}_x\text{O}_y/\text{InP}$ HSs after TO at 500 and 530 °C, 60 minutes

Sample, TO mode	Interplane distance, d_{hkl}	Defined phase
SnO_2/InP (530 °C)	5.5324	$\text{In}(\text{PO}_3)_3$
	3.6897; 3.5745	$\text{Sn}_3(\text{PO}_4)_2$
	3.0299	InSn_4
	2.932	InP
	1.4814	In_2O_3
	1.5074	InPO_4
	1.4668	P_2O_5
TiO_2/InP (500 °C)	2.9305; 1.4652	InP
	2.9213; 1.5256	In_2O_3
	1.5157; 1.4815; 1.3976	TiO_2
	1.5109; 1.4863	Ti_2O_3
$\text{V}_2\text{O}_5/\text{InP}$ (500 °C)	4.999; 1.729	In_2O_3
	3.414; 4.392	V_2O_5
	1.468; 2.935	InP
	2.480; 2.244	V_2O_3
	2.013	VO_2
	1.451; 3.709	InPO_4
MnO_2/InP (500 °C)	4.999; 1.729	In_2O_3
	3.108; 2.005	MnO_2
	1.468; 2.935	InP
	2.494; 2.110	Mn_2O_3
	1.451; 3.709	InPO_4

**Fig. 2.** STM image of the surface of the $\text{V}_2\text{O}_5(35 \text{ nm})/\text{GaAs}(100)$ samples (TO 500 °C, 50 min) (a) and AFM image of the surface of the $\text{MnO}_2(34 \text{ nm})/\text{GaAs}(100)$ sample (TO 500 °C, 60 min) (b). The scanning areas are 1.6×1.6 and $3 \times 3 \mu\text{m}^2$, respectively. The thickness of oxide films (LE) is 83 nm and 77 nm, respectively

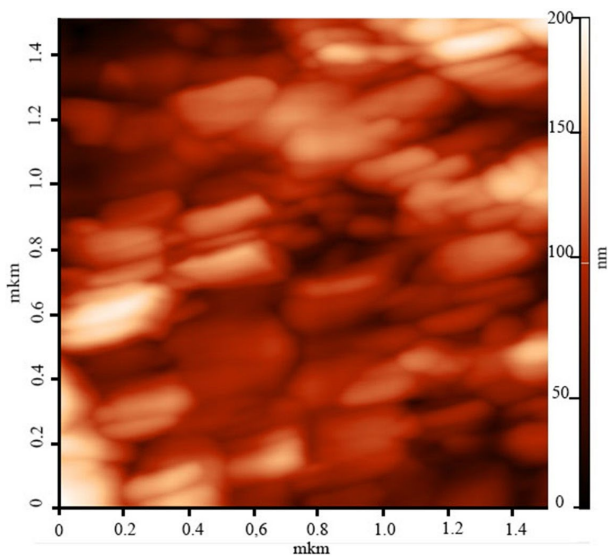


Fig. 3. AFM image of the surface of the $\text{MnO}_2/\text{GaAs}(100)$ sample (TO 500 °C, 180 min). The scanning area is $1.5 \times 1.5 \mu\text{m}^2$. The thickness of the oxide film (LE, SE) is 232 nm

film of 120 nm) (Fig. 4), the surface of the formed film became rough with pronounced structural elements (lines, bends, grains of an average size of 30 nm). After 60 minutes of oxidation of the MnO_2/InP HS at 530 °C (film thickness of 76 nm), the relief height did not exceed 20 nm, and the surface was characterised by a grain structure with an average size of 55 nm [13].

When potential chemostimulators, which are able to modify the composition of the growing films (SnO_2 , TiO_2 [14]), were applied on InP, which resulted in the formation of phosphates of the introduced element (see Table 4), fairly coarse-grained films with a grain diameter of 100–700 nm, depending on the synthesis mode, and a relief height of 20–40 nm were formed at 500–550 °C in 60 minutes (Fig. 5).

The comparison of the morphology of TiO_2/InP samples which were thermally oxidised at temperatures of 500 °C (Fig. 6a) and 530 °C (Fig. 6b) for 60 minutes showed that at higher temperatures the film surface had a more pronounced grain structure but with a smaller height difference.

Table 5 summarises the data that illustrate the effect of the substrate type on the surface morphology of the films grown by thermal oxidation of the corresponding HSs.

It can be seen that films formed on InP generally have a more uniform relief than those

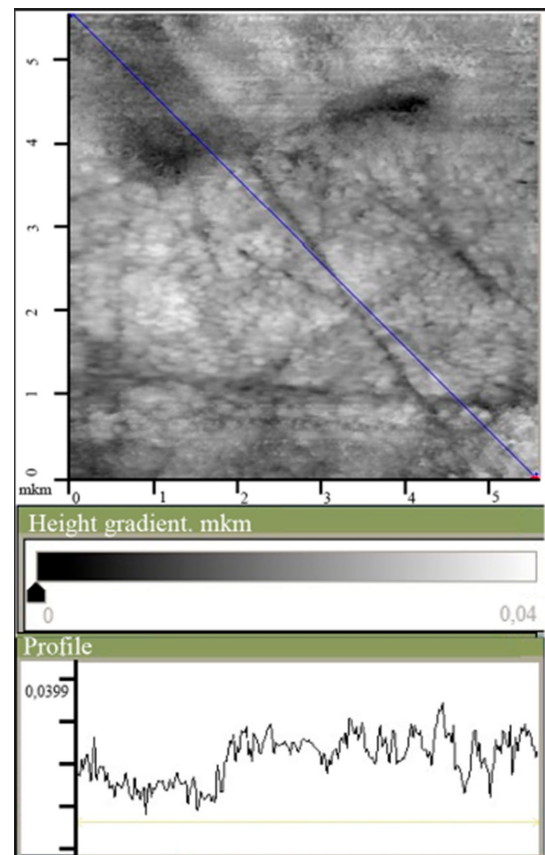


Fig. 4. STM image and surface profile of the $\text{V}_2\text{O}_5/\text{InP}$ sample (TO 530 °C, 60 min). The scanning area is $5.5 \times 5.5 \mu\text{m}^2$. The thickness of the oxide film (LE) is 120 nm

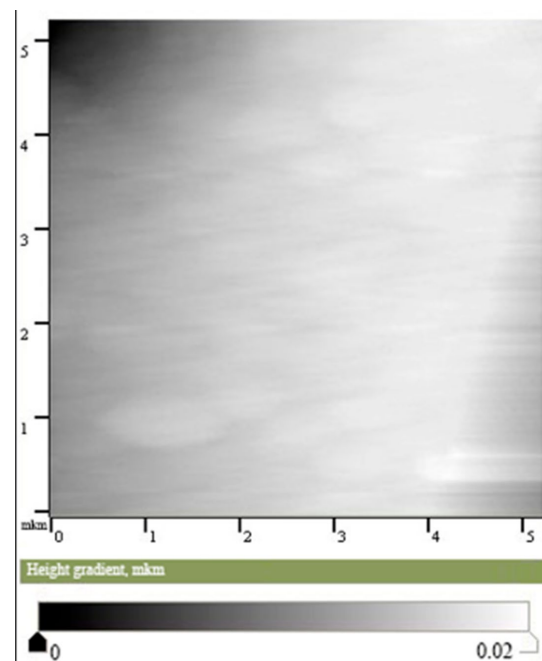


Fig. 5. STM image of the surface of the SnO_2/InP sample (TO 550 °C, 60 min). The scanning area is $5.2 \times 5.2 \mu\text{m}^2$. The thickness of the oxide film (LE) is 90 nm

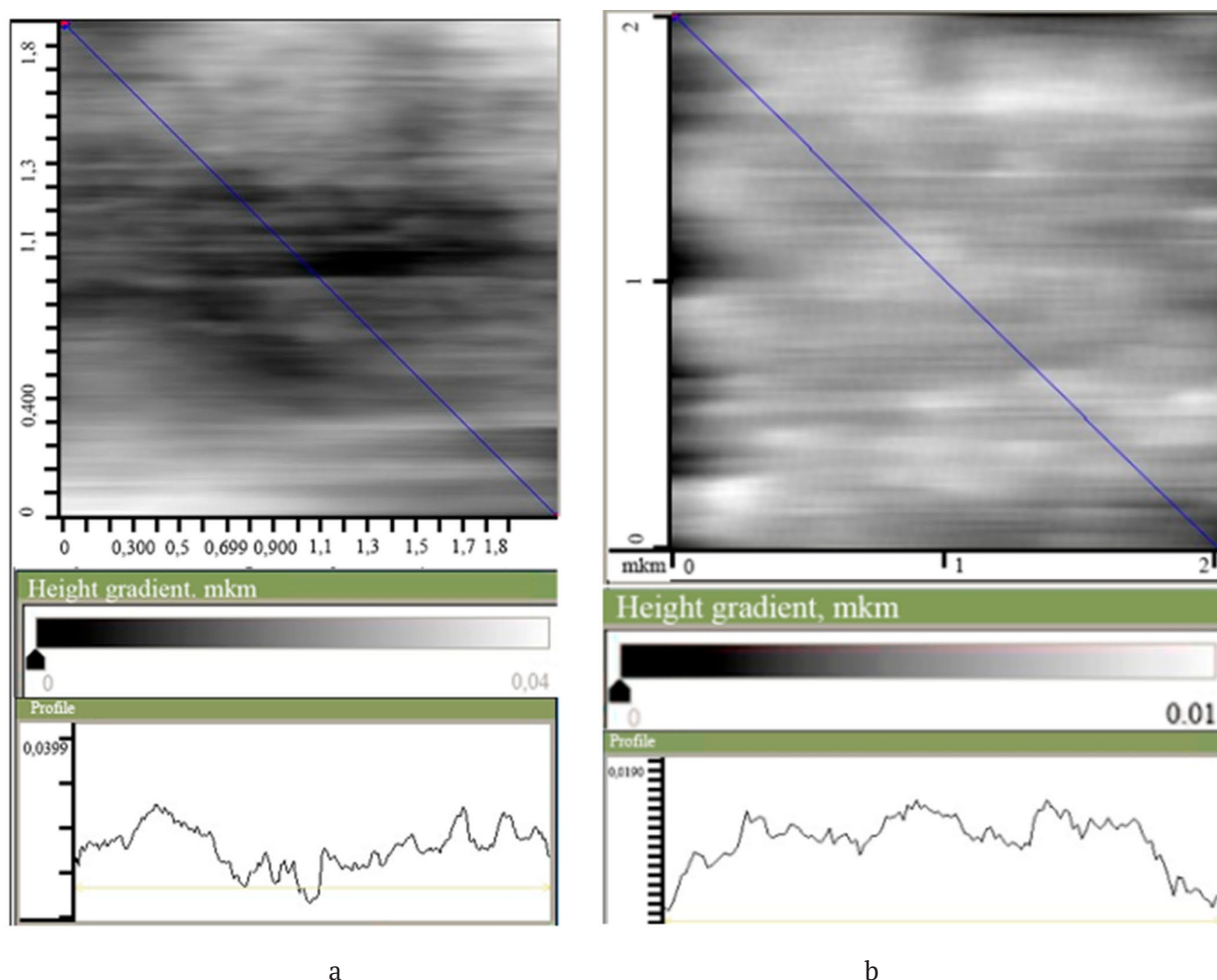


Fig. 6. STM image and the surface profile of the TiO_2/InP samples (TO 500 °C, 60 min) (a) and TiO_2/InP (TO 530 °C, 60 min) (b). The scanning areas are $2 \times 2 \mu\text{m}^2$. The thickness of the formed films (LE) is 50 nm and 55 nm, respectively

Table 5. Surface characteristics (STM, AFM) of $\text{Me}_x\text{O}_y/\text{InP}$ and $\text{Me}_x\text{O}_y/\text{GaAs}$ HSs depending on the type of substrate

Sample	TO mode	Scanning area, μm^2	Relief height, nm	Average grain size, nm
$\text{V}_2\text{O}_5/\text{InP}$	550 °C, 60 min	5.5×5.5	40	30
$\text{V}_2\text{O}_5/\text{GaAs}(100)$	500 °C, 50 min	1.6×1.6	9	150
MnO_2/InP	530 °C, 60 min	5.2×5.2	20	50
$\text{MnO}_2/\text{GaAs}(100)$	500 °C, 60 min	3×3	70	360

formed on GaAs; they also have smaller grains. Such films have a thickness corresponding to the nanoscale range and a nanodispersed structure. The TiO_2/InP HS (Table 6) can be used as an example to trace the effect of temperature at the same duration of the process on the surface morphology of the films. As the table shows, a higher temperature contributes to the smoothing of the surface relief, however, the grain size in

the lateral direction increases more than twice.

The physicochemical nature of the oxides in the deposited layers has the most significant effect on film structuring (Table 7). HSs with oxide layers, which perform the functions of a modifier and have a noticeable chemostimulating effect on the process of thermal oxidation (V_2O_5 , MnO_2) [10–13], for the same semiconductor (InP) produce nanosized and nanostructured films. In

Table 6. Surface characteristics (STM, AFM) of $\text{Me}_x\text{O}_y/\text{InP}$ HSs depending on the thermal oxidation mode

Sample	TO mode	Scanning area, μm^2	Relief height, nm	Average grain size, nm
TiO_2/InP	500 °C, 60 min	2×2	25	90
TiO_2/InP	530 °C, 60 min	2×2	12	250

Table 7. Surface characteristics (STM, AFM) of $\text{Me}_x\text{O}_y/\text{InP}$ HSs depending on the type of chemostimulator

Sample	TO mode	Scanning area, μm^2	Relief height, nm	Average grain size, nm
SnO_2/InP	550 °C, 60 min	5.2×5.2	20	400
TiO_2/InP	530 °C, 60 min	2×2	12	250
$\text{V}_2\text{O}_5/\text{InP}$	550 °C, 60 min	5.5×5.5	40	30
MnO_2/InP	530 °C, 60 min	5×5	20	50

the case of the solely modifying effect on the composition of the formed films (SnO_2/InP , TiO_2/InP), even at a relatively small height of the relief, the films are coarse-grained, with a lateral grain size of up to 400 nm.

4. Conclusion

The targeted selection of compounds, orientations of the A^3B^5 semiconductor substrate, and the oxidation conditions make it possible to vary the thickness and surface morphology of the films. The introduction of the most effective chemostimulator-modifiers (V_2O_5 , MnO_2) of thermal oxidation on the surface of GaAs and InP, as compared to less efficient chemostimulator-modifiers (SnO_2 , TiO_2), causes the formation of smoother films with a nanodispersed surface structure. The smoothing of the surface relief of oxide films is also promoted by a higher temperature of the oxidation process.

Author contributions

All authors made an equivalent contribution to the preparation of the publication.

Conflict of interests

The authors declare that they have no known competing financial interests or personal relationships that could have influenced the work reported in this paper.

References

1. Oktyabrsky S., Peide Ya. *Fundamentals of III-V Semiconductor MOSFETs*. Boston: Springer-Verlag; 2010. 445 p. <https://doi.org/10.1007/978-1-4419-1547-4>
2. Alferov Zh. I., Zubov F. I., Cirilin G. E., Zhukov A. E., Shchavruk N. V., Pavlov A. Yu., Ponomarev D. S.,

Klochkov A. N., Khabibullin N. A., Maltsev P. P. The first terahertz quantum-cascade laser fabricated in Russia. *Nano- and Microsystem Technology*. 2017;19(5): 259–265. <https://doi.org/10.17587/nmst.19.259-265>

3. Sheng S. Li. *Semiconductor physical electronics*. New York: Springer-Verlag; 2006. 708 p. <https://doi.org/10.1007/0-387-37766-2>

4. Ünlü H., Horing N. J. M., Dabowski J. *Low-dimensional and nanostructured materials and devices*. Springer Science LCC; 2015. 674 p. <https://doi.org/10.1007/978-3-319-25340-4>

5. Khan S. B., Akhtar K. *Photocatalysts: Applications and attributes*. IntechOpen; 2019. 143 p. <https://doi.org/10.5772/intechopen.75848>

6. Mittova I. Ya., Sladkoptsev B. V., Mittova V. O. Nanoscale semiconductor and dielectric films and magnetic nanocrystals - new directions of development of the scientific school of Ya. A. Ugai "Solid state chemistry and semiconductors". Review. *Kondensirovannye sredy i mezhfaznye granitsy = Condensed Matter and Interphases*. 2021;23(3): 309–336. <https://doi.org/10.17308/kcmf.2021.23/3524>

7. Moshnikov V. A., Alexandrova O. A. *Nanostructured oxide materials in modern micro-, nano- and optoelectronics*. Saint Petersburg: SPbGETU «LETI» Publ.; 2017. 266 p. (In Russ.)

8. Mittova I. Ya. Influence of the physicochemical nature of chemical stimulators and the way they are introduced into a system on the mechanism of the thermal oxidation of GaAs and InP. *Inorganic Materials*. 2014;50(9): 874–881. <https://doi.org/10.1134/s0020168514090088>

9. Tomina E. V., Mittova I. Ya., Sladkoptsev B. V., Kostyukov V. F., Samsonov A. A., Tretyakov N. N. Thermal oxidation as a method of formation of nanoscale functional films on $\text{A}^{\text{III}}\text{B}^{\text{V}}$ semiconductors: chemostimulated influence of metal oxides: overview. *Kondensirovannye sredy i mezhfaznye granitsy = Condensed Matter and Interphases*. 2018;20(2): 184–

203. (In Russ., abstract in Eng.) <https://doi.org/10.17308/kcmf.2018.20/522>

10. Mittova I. Ya., Tomina E. V., Lapenko A. A., Sladkopevtsev B. V. Catalytic action of vanadium and its oxide (V) in the processes of oxidation of A^{III}B^V semiconductors. *Nanosystems: Physics, Chemistry, Mathematics*. 2012;3(2): 116–138. (In Russ.) Available at: <https://www.elibrary.ru/item.asp?id=17881315>

11. Tretyakov N. N., Mittova I. Ya., Sladkopevtsev B. V., Agapov B. L., Pelipenko D. I., Mironenko S. V. Surface morphology, composition, and structure of nanofilms grown on InP in the presence of V₂O₅. *Inorganic Materials*. 2015;51(7): 655–660. <https://doi.org/10.1134/S002016851507016X>

12. Mittova I. Ya., Sladkopevtsev B. V., Tomina E. V., Samsonov A. A., Tretyakov N. N., Ponomarenko S. V. Preparation of dielectric films via thermal oxidation of MnO₂/GaAs. *Inorganic Materials*. 2018;54(11): 1085–1092. <https://doi.org/10.1134/S0020168518110109>

13. Tretyakov N. N., Mittova I. Ya., Sladkopevtsev B. V., Samsonov A. A., Andreenko S. Yu. Effect of a magnetron-sputtered MnO₂ layer on the thermal oxidation kinetics of InP and the composition and morphology of the resultant films. *Inorganic Materials*. 2017;53: 65–71. <https://doi.org/10.1134/S0020168517010174>

14. Mittova I. Ya., Kostyukov V. F., Ilyasova N. A., Sladkopevtsev B. V., Samsonov A. A. Modification of nanoscale thermal oxide films formed on indium phosphide under the influence of tin dioxide. *Nanosystems: Physics, Chemistry, Mathematics*. 2020;11(1): 110–116. <https://doi.org/10.17586/2220-8054-2020-11-1-110-116>

15. Bersirova O. L., Bruk L. I., Dikusar A. I., Karaman M. I., Sidelnikova S. P., Simashkevich A. V., Sherban D. A., Yapontseva Yu. S. Thin films of titanium and tin oxides and semiconductor structures on their basis obtained by pyrolytic pulverization: Preparation, characterization, and corrosion properties. *Surface Engineering and Applied Electrochemistry*. 2007;43(6): 443–452. <https://doi.org/10.3103/S1068375507060075>

16. Diebold U. The surface science of titanium dioxide. *Surface Science Reports*. 2003;48(5–8): 53–229. [https://doi.org/10.1016/S0167-5729\(02\)00100-0](https://doi.org/10.1016/S0167-5729(02)00100-0)

17. Khoroshikh V. M., Bilous V. A. Titanium dioxide films for photocatalysis and medicine. *FIP FIP PSE*. 2009;7(3): 223–238. (In Russ.) Available at: <http://dspace.nbuv.gov.ua/bitstream/handle/123456789/7978/07-Khoroshikh.pdf?sequence=1>

18. Sangwal K. *Etching of crystals: Theory, experiment, a. application*. Amsterdam: North-Holland Physics Publishing; 1987. 496 p.

19. Acosta D. R., Martínez A., Magaña C. R., Ortega J. M. Electron and Atomic Force Microscopy

studies of photocatalytic titanium dioxide thin films deposited by DC magnetron sputtering. *Thin Solid Films*. 2005;490(2): 112–117. <https://doi.org/doi:10.1016/j.tsf.2005.04.067>

20. Kostyukov V. F., Mittova I. Ya., Shvets V. A., Tomina E. V., Sladkopevtsev B. V., Tret'yakov N. N. Spectral ellipsometry study of thin films grown on GaAs by chemically stimulated thermal oxidation. *Inorganic Materials*. 2014;50(9): 882–887. <https://doi.org/10.1134/S0020168514090052>

21. Shvets V. A., Rykhliitskii, S. V., Mittova, I. Ya., Tomina E. V. Analysis of the optical and structural properties of oxide films on InP using spectroscopic ellipsometry. *Technical Physics*. 2013;58: 1638–1645. <https://doi.org/10.1134/S1063784213110248>

22. Spesivtsev E. V., Rykhliitskii S. V., Shvets V. A. Development of methods and instruments for optical ellipsometry at the Institute of Semiconductor Physics of the Siberian Branch of the Russian Academy of Sciences. *Optoelectronics Instrumentation and Data Processing*. 2011;47(5): 419–425. <https://doi.org/10.3103/S8756699011050219>

23. Nakamoto K. *Infrared and Raman spectra of inorganic and coordination compounds*. New York: John Wiley; 1986. 479 p.

24. Vorobyev N. I. *Atlas of infrared spectra of phosphates. Double condensed phosphates*. Minsk: Foundation for Fundamental Research Publ.; 1993. 250 p. (In Russ.)

Information about authors

Anastasia S. Kovaleva, 2nd year master's degree student, Voronezh State University (Voronezh, Russian Federation).

<https://orcid.org/0000-0002-0350-8518>
nkovaleva.vsu@yandex.ru

Boris V. Sladkopevtsev, PhD in Chemistry, Associate Professor at the Department of Materials Science and Nanosystem Technologies, Voronezh State University (Voronezh, Russian Federation).

<https://orcid.org/0000-0002-0372-1941>
dp-kmins@yandex.ru

Alexey A. Samsonov, PhD in Chemistry, Lead Engineer at the Department of Materials Science and Nanosystem Technologies, Voronezh State University (Voronezh, Russian Federation).

<https://orcid.org/0000-0002-9338-815X>
samsonjr@mail.ru

Svetlana I. Alferova, PhD in Chemistry, Associate Professor at the Department of Chemistry, Voronezh State Pedagogical University (Voronezh, Russian Federation).

<https://orcid.org/0000-0001-7304-5988>
alferovasvet53@mail.ru

Danila G. Kovalev, 2nd year master's degree student, Voronezh State University (Voronezh, Russian Federation).

<https://orcid.org/0000-0003-2265-1579>

dkovalev754@gmail.com

Sergey A. Titov, student, Voronezh State University (Voronezh, Russian Federation).

<https://orcid.org/0000-0001-6322-8174>

donatedmaster@mail.ru

Nikita D. Priakhin, student, Voronezh State University (Voronezh, Russian Federation).

<https://orcid.org/0000-0002-8453-2412>

revan19_91@mail.ru

Irina Ya. Mittova, DSc in Chemistry, Professor at the Department of Materials Science and Nanosystems Technologies, Voronezh State University (Voronezh, Russian Federation).

<https://orcid.org/0000-0001-6919-1683>

imittova@mail.ru

Received December 15, 2021; approved after reviewing December 21, 2021; accepted February 15, 2022; published online March 25, 2022.

Translated by Irina Charychanskaya

Edited and proofread by Simon Cox